Excited Wannier excitons in half-space geometry

I. Balslev
Fysisk Institut, Odense Universitet, Campusvej 55, DK-5230 Odense M, Denmark
(Received 4 February 1983)

The two-body problem of an electron-hole pair near a crystal surface is solved within the framework of the adiabatic approximation which is valid for small reduced-mass to total-mass ratios. Wave functions and eigenenergies associated with the relative motion are calculated as a function of center-of-mass depth for states derived from $n=2$ excitons. Only optically allowed states are studied, namely the two $2s\,2p_z$ admixtures which become two nondegenerate states near the surface. The computations are based on discretization in space with the use of the finite-element method.

I. INTRODUCTION

Great interest has been devoted to the influence of a crystal surface on Wannier excitons.[1–14] The predominant intrinsic surface effect conventionally described by the exciton-free layer[2] is due to the short-range forces acting on the electron and the hole.[6,7] So far it has not been possible to perform an accurate theoretical treatment of the relevant two-body problem, but some insight is gained by applying the adiabatic approximation[6,7] or studying a one-dimensional model.[13,14]

In contrast to the above-mentioned works the present paper deals with the influence of a surface on higher-lying exciton states, specifically those derived from the $n=2$ bulk exciton state. Unlike $n=1$ states, the $n=2$ and higher states are sensitive to the reduction of spatial symmetry near a surface. This leads to level splitting in the adiabatic approximation. A further complication of higher exciton states is that the variational calculation used for $n=1$ excitons[6,7] is inadequate.

In the search for alternative computational methods it turned out to be extremely difficult (if not impossible) to avoid the brute-force method based on discretization in space. Thus the author was unable to find a suitable series expansion based on nonlocalized basis functions fulfilling the appropriate boundary conditions. With discretization in space it was advantageous to use the finite-element method[15] rather than simple difference equations derived from the wave equation. Methods based on discretization in space, particularly the finite-element method, are rarely used in quantum mechanics but are quite common when solving engineering problems in heat conduction, diffusion, fluid flow, electromagnetism, etc. The present treatment of the $n=2$ excitons applies the adiabatic approximation[6,7] and focuses on eigenenergies and eigenfunctions associated with the relative motion. These quantities can be used in a polariton model because they define the resonance frequency and oscillator strength as functions of depth below the surface.[7,11,14,16]

II. EXCITON NEAR A SURFACE

Let us consider a semi-infinite crystal at $z>0$. The electron-hole wave function $\Psi(\vec{r}_e,\vec{r}_h)$ and the exciton energy E (relative to the band gap) are determined by

$$\left[-\frac{\hbar^2}{2m_e}\nabla_e^2-\frac{\hbar^2}{2m_h}\nabla_h^2-\frac{e^2}{4\pi\epsilon\,|\,\vec{r}_e-\vec{r}_h\,|}+V_s-E\right]\Psi=0\ . \tag{1}$$

Here m_e and m_h are the effective masses of electron and hole, respectively, ϵ is the dielectric constant, and V_s is a potential due to the surface at $z=0$. As in Ref. 7 the following two intrinsic contributions to V_s are considered. (a) The image charge forces leading to

$$V_s=\frac{\epsilon-\epsilon_0}{\epsilon+\epsilon_0}\frac{e^2}{4\pi\epsilon}\left[\frac{1}{4z_e}+\frac{1}{4z_h}-\frac{1}{[(x_e-x_h)^2+(y_e-y_h)^2+(z_e+z_h)^2]^{1/2}}\right], \tag{2}$$

and (b) short-range forces the effect of which can be described by the boundary conditions

$$\Psi=0 \quad \text{for } z_e\le 0\ , \qquad \Psi=0 \quad \text{for } z_h\le 0. \tag{3}$$

With a general mass ratio Eq. (1) is too complicated to handle. We therefore apply the adiabatic approximation valid in the limit $\mu/M\ll 1$, where μ and M are the reduced mass and total exciton mass, respectively. Then

$$\Psi=g_{p,m}(\vec{r};Z)G(\vec{R})\ , \tag{4}$$

where $\vec{r}=(x,y,z)$ and $\vec{R}=(X,Y,Z)$ are relative and center-of-mass coordinates, respectively, and $g_{p,m}$ and G are solutions to

$$\left[-\frac{\hbar^2}{2\mu}\nabla_{\vec{r}}^2-\frac{e^2}{4\pi\epsilon r}+V_s(\vec{r};Z)-E_p(Z)\right]g_{p,m}(\vec{r};Z)=0 \tag{5}$$

and

$$\left[-\frac{\hbar^2}{2M}\nabla^2_{\vec{R}}+E_p(Z)-E\right]G(\vec{R})=0\ . \tag{6}$$

Here p counts the eigenenergies $E_p(Z)$ and m is the magnetic quantum number (with quantization along the z axis). In the bulk ($Z\to\infty$), p should be replaced by the hydrogenic quantum numbers n,l. For simplicity the present analysis will be restricted to $m=0$ states with $g_p(\vec{r};Z)\equiv g_{p,0}(\vec{r};Z)$. The relevant solutions to Eq. (5) are those fulfilling the boundary conditions in relative space given by

$$\begin{aligned} &g_p(\vec{r};Z)=0 \quad \text{for } z\le -ZM/m_h\ , \\ &g_p(\vec{r};Z)=0 \quad \text{for } z\ge ZM/m_e\ . \end{aligned} \tag{7}$$

Considering only closed-orbit excitons ($E_p(Z)<0$), g_p goes to zero exponentially for $|\vec{r}|$ going to infinity. Therefore, in a numerical treatment it is appropriate to use the boundary condition

$$g_p(\vec{r};Z)=0 \quad \text{for } |\vec{r}|\ge r_{\max}\ , \tag{8}$$

where $r_{\max}$ is chosen sufficiently large.

III. NUMERICAL METHOD

An approximate solution to Eq. (5) can be expressed as

$$g_p(\vec{r};Z)=\sum_i C_{p,i}(Z)v_i(r,\theta)\ , \tag{9}$$

where (r,θ,φ) are spherical coordinates in relative space, $C_{p,i}(Z)$ are expansion coefficients, and $v_i(r,\theta)$ are element functions of the finite-element method. The following bilinear form of $v_i(r,\theta)$ has been chosen:

$$v_i(r,\theta)=\begin{cases} 0 \quad \text{for } |\theta-\theta_i|>\Delta\theta,\ |r-r_i|>\Delta r \\ \left|\dfrac{r-r^*}{r_i-r^*}\,\dfrac{\theta-\theta^*}{\theta_i-\theta}\right| \quad \text{otherwise}\ , \end{cases} \tag{10}$$

where r_i,θ_i are coordinates about which $v_i(r,\theta)$ are localized, Δr and $\Delta\theta$ are increments between neighboring points, and r^*,θ^* are corner coordinates $r_i\pm\Delta r,\theta_i\pm\Delta\theta$ closest to r,θ. Figure 1 shows the typical choice of coordinates r_i,θ_i. Note that the conditions (7) are incorporated by omitting points outside and on the zigzag curve shown. With the use of form (10) one obtains $v_i(r_j,\theta_j)=\delta_{ij}$ and that $C_{p,i}(Z)$ are approximate values of g_p at (r_i,θ_i). According to Ref. 15 the coefficients $C_{p,i}(Z)$ can be calculated from the equations

$$\sum_i C_{p,i}(Z)M_{ij}(Z)=0\ , \tag{11}$$

where

$$M_{ij}(Z)=\int\left[\frac{\hbar^2}{2\mu}\vec{\nabla}v_i\cdot\vec{\nabla}v_j+\left[V_s-\frac{e^2}{4\pi\epsilon r}-E_p(Z)\right]v_iv_j\right]d^3r\ . \tag{12}$$

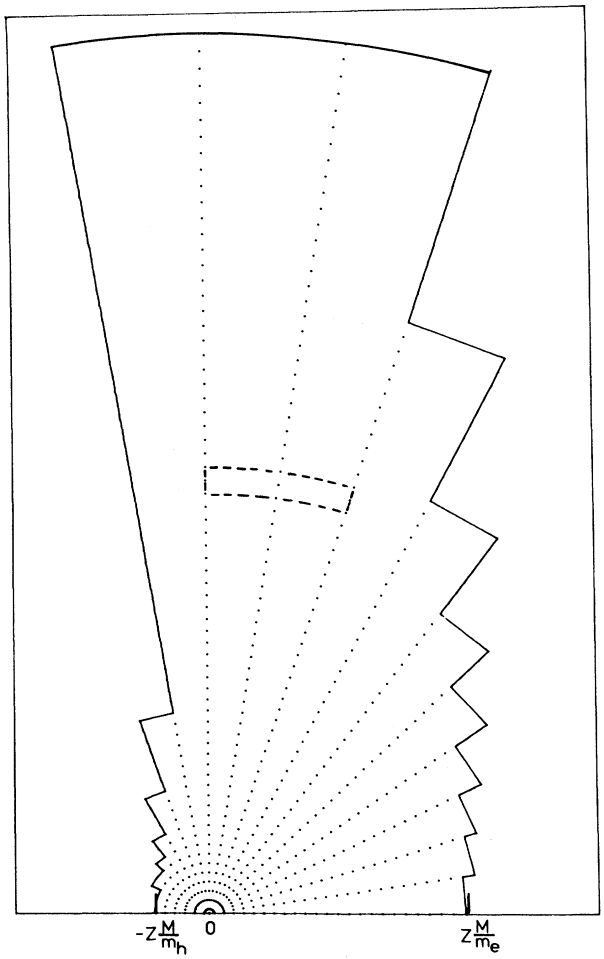

FIG. 1. Domain in the x-z plane of relative space showing the boundary and elementary points (r_i,θ_i) used in the finite-element method. Dots are elementary points, dashed inset is the limitation of a single basis function $v_i(r,\theta)$, and solid lines indicate the curves on which the approximate function $f(\vec{r};Z;E_0)$ of Eq. (16) is zero.

Equation (11) is a generalized eigenvalue problem which in case of closely lying eigenvalues is somewhat complicated to handle. In the present treatment it was preferred to solve the following modification of Eq. (5):

$$\left[-\frac{\hbar^2}{2\mu}\nabla^2_{\vec{r}}-\frac{e^2}{4\pi r}+V_s(\vec{r};Z)-E_0\right]f(\vec{r};Z;E_0)=\frac{\delta(r-r_0)}{4\pi r_0^2}\ . \tag{13}$$

where E_0 (as Z) is a free parameter and r_0 in the source term $\delta(r-r_0)$ is much smaller than the exciton Bohr radius a_B.[17] Expanding $f(\vec{r};Z,E_0)$ in eigenfunctions $g_p(\vec{r};Z)$ one obtains

$$f(\vec{r};Z;E_0)=\sum_p\frac{g_p(\vec{r};Z)\int g_p(\vec{r}';Z)\delta(r'-r_0)d^3r'}{4\pi r_0^2[E_p(Z)-E_0]}\ . \tag{14}$$

Here we have used that all eigenstates $g_p(\vec{r};Z)$ are nondegenerate. For $r_0 \to 0$ we may write[18]

$$f(\vec{0};Z;E_0) \approx \sum_p \frac{g_p^2(\vec{0};Z)}{E_p(Z)-E_0} . \tag{15}$$

It is seen that dependence on E_0 of $f(\vec{0};Z;E_0)$ is characterized by poles at the eigenstates unless $g_p(\vec{0};Z)=0$. $f(\vec{0};Z;E_0)$ has a direct physical meaning in case of optical excitonic reasonances. Then, in the limit $\mu/M \to 0$, $f(\vec{0};Z;E_0)$ is proportional to the excitonic susceptibility at the depth Z and at a frequency $(-E_0)/\hbar$ below the gap frequency. In the determination of $f(\vec{r};Z;E_0)$ we write

$$f(\vec{r};Z;E_0) = \sum_i C^*{}_i(Z,E_0) v_i(r,\theta) \tag{16}$$

and

$$\sum_i C_i^*(Z,E_0) M_{ij}^*(Z,E_0) = Q_j^* , \tag{17}$$

where

$$M_{ij}^*(Z,E_0) = \int \left[\frac{\hbar^2}{2\mu} \vec{\nabla} v_i \cdot \vec{\nabla} v_j + \left(V_s - E_0 - \frac{e^2}{4\pi\epsilon r} \right) v_i v_j \right] d^3r \tag{18}$$

and

$$Q_i^* = \int v_i \delta(r - r_0) d^3r . \tag{19}$$

Equation (17) represents linear equations with solutions for all Z and $E_0 \neq E_p(Z)$.

The exact matrix elements M_{ij}^* were calculated analytically except for the contribution involving V_s. For this the approximation

$$\int V_s v_i v_j \, d^3r \approx V_s(\tfrac{1}{2}\vec{r}_i + \tfrac{1}{2}\vec{r}_j;Z) \int v_i v_j \, d^3r \tag{20}$$

was used. The region bounded by $0 < r < \Delta r$ and $0 < \theta < \pi$ was covered by a single-element function v_0 given by

$$v_0 = \frac{\Delta r - r}{\Delta r} . \tag{21}$$

Inside this region the Coulomb potential is singular, but the matrix elements involving the element v_0 are finite.

IV. RESULTS AND DISCUSSION

The calculations were performed with $r_{\max} = 16a_B$, $\Delta r = 0.3a_B$, $\Delta\theta = 0.15$ rad, $r_0 = 0.3a_B$, $\mu/M = 0.1$, and $\epsilon/\epsilon_0 = 8$. It was checked that the solutions for $f(\vec{0};Z;E_0)$ were reasonably independent of the computational input variables $\Delta r, \Delta\theta, r_{\max}$. Bulk solutions (calculated with $Z > r_{\max}$, $\Delta r = 0.3a_B$, and $\Delta\theta = \pi$) revealed poles of $f(\vec{0};\infty;E_0)$ for $E_0 = -E_x$ and $-E_x/4$ (E_x is the exciton Rydberg) in agreement with the analytical result for hydrogen. The interest was focused on the $n=2$ level, so the linear equations [(Eq. 17)] were solved for about 200 different values of (Z,E_0) in the range $0.5a_B < Z < 10a_B$ and

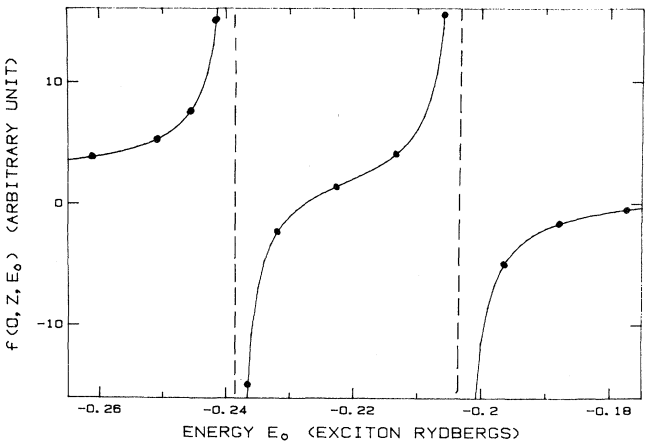

FIG. 2. Computed values of $f(\vec{0};Z;E_0)$ for $Z = 6.3a_B$. Dots are computed points while solid lines are drawn as guide for the eye.

$-0.33E_x < E_0 < -0.14E_x$. A typical dependence on E_0 of $f(\vec{0};Z;E_0)$ is shown in Fig. 2 (with $Z = 6.3a_B$) where two poles are clearly seen. Following the energies $E_p(Z)$ of the poles to lower and higher values of Z one obtains the full dependence of $E_p(Z)$ as shown in Fig. 3. The energies of the two sublevels in the investigated range are well represented by the expression

$$E_p(Z)/E_x = \begin{cases} -\frac{1}{4} + 0.26\exp(-Z/2a) \\ -\frac{1}{4} + 1.1\exp(-Z/2a) \end{cases} \tag{22}$$

The two residues of $f(\vec{0};Z;E_0)$ at $E_0 = E_p(Z)$ turned out to be comparable and approximately independent of Z. Thus the oscillator strength of the bulk $n=2$ excitonic resonance is essentially evenly distributed on the two sublevels.

The findings shown in Figs. 2 and 3 agree well with symmetry arguments: The $2p\,2s$ bulk level splits near a surface into a doubly degenerate $m = \pm 1$ level and two

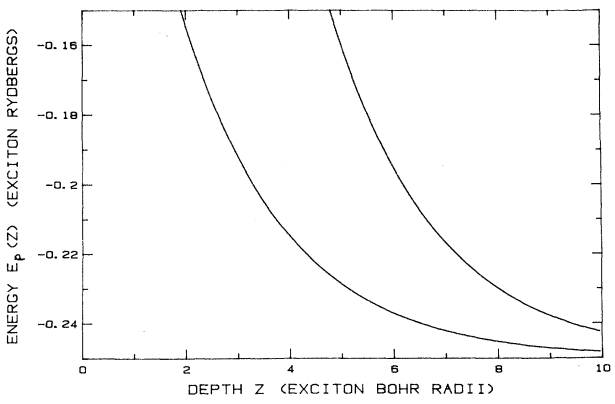

FIG. 3. Energy shifts $E_p(Z)$ of the two $m=0$ sublevels derived from the $n=2$ bulk exciton with $\mu/M = 0.1$ and $\epsilon/\epsilon_0 = 8$.

nondegenerate $2s$-$2p_z$ admixtures with finite values of $g_p(\vec{0};Z)$. The energy shift would have an inverse cubic Z dependence if image charge forces were dominant. The fact that the shifts are proportional to $\exp(-Z/na_B)$ indicates that these are mainly due to cutoff forces (as is the case also for $n=1$ excitons in the hydrogen limit[7]).

V. CONCLUSION

The present study of exciton states in half-space geometry revealed a well-defined splitting of the $n=2$ level. Among the applications of the result is the calculation of normal incidence reflectance spectra based on a polariton model including spatial dispersion.[16]

The results of the present work were obtained by the finite-element method, an unconventional computational technique in quantum mechanics. The method proved very efficient in the solution of a problem with two independent spatial variables (r,θ). It is under consideration to extend the calculation to include Z as a third spatial integration variable in order to avoid the adiabatic approximation. In that case the polariton theory developed by Stahl[13] should be used as a basis for the numerical treatment.

ACKNOWLEDGMENTS

The author is deeply indebted to E. Christiansen, Department of Mathematics, Odense University, and A. Stahl, Rheinisch-Westfälische Technische Hochschule, Aachen, for many valuable discussions.

[1]S. I. Pekar, Zh. Eksp. Teor. Fiz. 33, 1022 (1957) [Sov. Phys.—JETP 6, 785 (1958)].
[2]J. J. Hopfield and D. G. Thomas, Phys. Rev. 132, 563 (1963).
[3]R. Zeyher, J. L. Birman, and W. Brenig, Phys. Rev. B 6, 4613 (1972).
[4]F. Evangelisti, A. Frova, and F. Patella, Phys. Rev. B 10, 4253 (1974).
[5]C. S. Ting, M. J. Frankel, and J. L. Birman, Solid State Commun. 17, 1285 (1975).
[6]S. Sakoda, J. Phys. Soc. Jpn. 40, 152 (1976).
[7]I. Balslev, Phys. Status Solidi B 88, 155 (1978).
[8]R. G. Ulbrich and C. Weisbuch, Phys. Rev. Lett. 38, 865 (1977).
[9]K. Hümmer and P. Gebhardt, Phys. Status Solidi B 85, 271 (1978).
[10]A. D'Andrea and R. Del Sole, Solid State Commun. 30, 143 (1979).
[11]I. Balslev, Solid State Commun. 39, 359 (1981).
[12]J. Lagois, Phys. Rev. B 23, 5511 (1981).
[13]A. Stahl, Phys. Status Solidi B 106, 575 (1981).
[14]I. Balslev and A. Stahl, Phys. Status Solidi B 111, 531 (1982).
[15]O. C. Zienkiewicz, *Finite Element Method in Engineering Science* (McGraw-Hill, London, 1971), p. 295.
[16]I. Balslev, Solid State Commun. 45, 661 (1983). [Here the expression for the energy shifts is incorrect. The correct shifts are given in Eq. (22) of the present paper.]
[17]A. Stahl and I. Balslev, Phys. Status Solidi B 113, 583 (1982).
[18]I. Egri and A. Stahl, Phys. Status Solidi B 96, K83 (1979).